ADAPTIVE ORBIT DETERMINATION FOR INTERPLANETARY SPACECRAFT

P. **Daniel** Burkhart[*]   **Robert H.** Bishop[†]

The interplanetary orbit determination problem has been tradition-
ally solved using least-squares techniques. Due to operational limi-
tations of this method, a Kalman filter approach has been proposed
for future missions. The proposed approach, known as the enhanced
filter, includes all spacecraft and measurement modeling states in the
filter. The goal of the enhanced filter is to increase the accuracy of
the navigation process while utilizing only radiometric (Doppler and
range) data. As an extension to the enhanced filter, an *adaptive* orbit
determination approach (based on the Magill filter bank) has been
developed here to process radiometric data. This adaptive approach
can be used as a systematic method for the determination of the
operational enhanced filter parameters, which are currently selected
using *ad* hoc methods. The first step in the development of the adap-
tive enhanced filter bank is the determination of the significant errors
in the problem, which is accomplished using covariance analysis to
develop an error budget. The Mars Pathfinder mission is utilized to
demonstrate the effectiveness of the adaptive enhanced filter bank in
determining variances for the process and measurement noise param-
eters based on the tracking data. The results for the range data case
show that the adaptive enhanced filter bank is effective in selecting
the process and measurement noise variances that match those used
to generate the data.. Results for the Doppler only case are not as
conclusive, due primarily to linearization errors.

1 Introduction

The orbit determination problem for interplanetary spacecraft involves the calcu-

lation of spacecraft states (i.e. position and velocity) and associated estimation

---

[*]Research Assistant, Department of Aerospace Engineering and Engineering Mechanics, The
University of Texas, Austin, Texas 78712; Member AI AA.
[†]Assistant Professor, Department of Aerospace Engineering and Engineering Mechanics, The
University of Texas, Austin, Texas 78712; Member AI AA.

uncertainty measures based on information received from measurements that are corrupted by various errors and random noise. The motivation for the work presented here is to improve the tools used to perform this task. Due to reductions in resources for navigation, the number of navigation team members will be significantly reduced for future missions. For many past missions, navigation teams had twenty members or mom, and current projections arc for three or four navigation team members. Combined with the navigation requirements for future missions, the amount of work required using current tracking methods is a major burden given the size of the navigation teams. One problem is the lack of a systematic method for determining appropriate values for the operational orbit determination filter. In current interplanetary navigation practice, the operational filter parameters, such as time constants, gravitational parameters, noise variances and system parameters, arc generally selected by trial and error based on experience and *computer simulation.* The filter parameters arc selected and the measurement data processed. Based on the simulation results, the filter parameters may be changed and the data processed again, or the current result may be accepted. During this iterative process, often the measurement data is de-weighted, resulting in estimation errors that are generally higher than the data requires. This *ad hoc* approach to filter tuning, in addition to failing to take full advantage of the inherent data accuracy, requires a large number of navigation team members to analyze the results from the data processing. Despite the success of this approach in the past, the current realities do not support its continued usc. The orbit determination task must be completed with fewer analysts, similar if not greater tracking accuracy requirements, and less tracking data, Therefore, a new methodology is required for opera.tional interplanetary navigation.

One constraint on any proposed solution to this problem is the utilization of

realistic error *sources* and models to accurately determine if the selected approach will be useful in the actual tracking process. In addition, the proposed solution must integrate easily with current navigation approaches. A Kalman filter approach will be used for future interplanetary missions, so the solution must be compatible with this recursive filter method. Due to the desire to minimize tracking station use, personnel costs and complexity, conventional Doppler and ranging data will be the data types used in this analysis. Finally, the approach must be implementable in a modular fashion. This is not only to avoid extensive modification of existing orbit determination software, but to allow the testing of other approaches in a smoother and less complicated fashion.

Along with the change from the least-squares filter to the Kalman filter, another major change in the current filtering practice being studied is reflected in the so-called *enhanced filter* [7]. Current practice involves modeling certain Earth platform and transmission media effects as *consider parameters* in the filter. In other words, these parameters arc allowed to affect the covariance of the estimated state, but arc not themselves estimated. The enhanced filter calls for inclusion of these parameters in the estimated state vector. When compared with current filtering practices, the result is increased accuracy in the state estimates [7]. This filtering strategy is currently being tested using real flight data from Galileo [8]. The enhanced Kalman filter is utilized in this paper.

The approach taken here is to utilize radiometric (Doppler and rang-c) data ant] to establish navigation improvements through the usc of *adaptive filtering* algorithms. 'J'here arc benefits to this approach, in addition to the systematic tuning of the operational filter. Suppose the process noise and/or data noise profile changes during the mission, for example, if the acceleration profile of the spacecraft changes significantly due to unmodeled venting. Then, the need for a non-labor

intensive method to detect changes in the data profile and to point to the source of the changes is clear. A Kalman filter bank (proposed here) will allow the analyst to model several filters simultaneously and directly compare the results automatically. The filter bank will determine which filter is opei sting optimally (where optimal is precisely defined later) with respect to the measurement dat a, thus helping the process of selecting the filter parameters. For the case where the process and/or measurement noise profile changes, the fil er bank can de-select a given filter and choose a different filter that more closely matches the current environment. In this way, in addition to the establishment of a systematic method to choose the operational filter parameters and to detect environmental changes, the orbit determination process can be completed with fewer team members, while potentially increasing the accuracy and timeliness of the resu Its.

The adaptive estimation solution described in this work solves the orbit determination problem very effectively given the real-world constraints. The adaptive filter can be used as an effective tool to assist the navigation engineer in selecting filter parameters, thus allowing a closer match of the filter parameters to the true values, leading to a potentially more accurate navigation solution. In addition, this method requires fewer hours of processing and analysis and allows a smaller group of analysts to determine accurate navigation solutions. More importantly, the long term objective of this study is to develop an adaptive filtering methodology that can be used for processing of actual mission data. It is shown in the subsequent analysis that this objective is successfully achieved.

Several methods were investigated in terms of ability to determine both process noise and measurement noise parameters and to be general enough to handle a time-varyin,g problem. Since the Kalman filter is already in use and is planned for future use for orbit determination, a method utilizing this approach is desirable for

implementation masons, It was found that the most desirable approach, in terms of these constraints, is the Magill Kalman filter bank [1]. This approach, also known as the Multiple Model Estimation Algorithm (MMEA), has been shown to be a practical algorithm in solving real-world problems [2], [3], [4]. One important-problem that can be solved most effectively using the Magill filter bank is that of hypothesis testing, which is to choose from a finite set of filters which hypothesized filter in the bank is the correct one [5], [6]. The Kalman filter bank implemented in this study is utilized as a hypothesis tester. The proposed methodology is a practical extension to current navigation practices for interplanetary spacecraft, In addition, the cost of integrating this approach with the current operational enhanced Kalman filter is minimal. The Kalman filter does not need to be modified in any way to implement this scheme. All that is required from the filter are pre-update measurement residuals and the covariance associated with these residuals at each data point, which are computed by the Kalman filter already. Finally, the assumptions that are required for application of the filter bank are the same that govern the use of a single Kalman filter. Thus, if the problem is formulated to work properly with the Kalman filter, the filter bank approach can be used without modification [(i].

The scenario chosen for this study is the Mars Pathfinder mission, scheduled for launch in December 1996. Specifics of the mission plan, including launch and arrival dates and the tracking scenario, are presented. A model was developed to represent accurately, but with moderate complexity, the actual data received by the filter during a mission. This model, consist ing of the spacecraft state, solar radiation pressure effects, small unmodeled acceleration effects, transmission media effects and Earth platform effects, is used to generate tracking data.

Various computational algorithms were studied to solve the adaptive filtering

problem, arid all the methods have the characteristic of increasing in computational cost as the number of filter parameters to be determined increases. For this reason, it is desirable to determine only the most critical error sources and to concentrate effort in the analysis on these areas. The less significant errors will remain as parameters in the filter, but will not participate in the adaptation. A special type of covariance analysis, or error budget analysis, is utilized here to catalog the contributions of particular error sources or error source groups to the overall estimation error. The error budget is presented for X-band range only, Doppler only, and Doppler plus range mca surement scenarios for the Mars Pathfinder mission.

Results are given for several different sets of noise parameters included in the adaptive scheme. Tracking schemes considered include range only and Doppler only. The main result is the demonstrated ability of the adaptive Kalman filter bank to determine the underlying measurement and process noise strengths. In addition, the results for the changing noise strengths case show the ability of the filter bank to detect environmental and/or spacecraft changes.

2 Mars Pathfinder Mission

The Mars Pathfinder mission is the first of a series of low-cost rapid turnaround science missions from NASA's Discovery Program. This mission will serve primarily as a demonstration of key technologies and concepts for use in future missions to Mars using scientific landers. in addition, Pathfinder includes a significant science payload. Investigations of the Martian atmosphere, surface meteorology, surface geology and morphology, and the elemental composition of Martian rocks arid soil are scheduled for Pathfinder. A free-ra)lging surface microrover is also part of the mission. This microrover will be deployed by Pathfinder to conduct technology related experiments and to serve as a mechanis n for instrument deployment [9].

The mission is scheduled for the 1996 Mars launch opportunity, with a 30 day launch window beginning on December 5, 1996 and ending on January 3, 1997. The arrival date at Mars is fixed at July 4, 1997, The transfer time will vary from 212 days to 182 days, depending on the actual launch date. The trajectory used for this study corresponds to the January 3, 1997 launch date. Upon arrival at Mars on July 4, 1997, the spacecraft will perform a direct entry into the Martian atmosphere. To achieve a landing, a parachute is deployed along with a rocket braking system and an airbag system. After landing the primary surface operations begin, which includes deployment of the microrover [9].

The interplanetary transfer phase of the Mars Pathfinder mission is under investigation here. The adaptive filtering approach proposed for the interplanetary navigation problem is not dependent on the Mars Pathfinder mission. The Mars Pathfinder scenario is chosen so that the adaptive filtering method could be tested using a realistic interplanetary mission. Epoch conditions are known for the spacecraft and the planets on March 5, 1997. The data arc used in this study lasts for 105 days from the epoch, or until June 18, 1997. A plot of the Earth, spacecraft and Mars trajectories is shown in Figure 1. The trajectory characteristics (the shaded portion of Figure 1) are detailed in Table 1. During interplanetary cruise, the scientific instruments will be checked but not used.

The interplanetary cruise portion of the mission begins approximately seven days after launch (L+7) and ends 15 days before encounter (M- 15). The main task during interplanetary cruise is to determine the required corrections to the trajectory to ensure the spacecraft arrives when and where it is scheduled. The nominal mission plan has four Trajectory Correction Maneuvers (TCM 's), if required. The first two maneuvers are scheduled at L+30 days (to correct for injection errors) and L+60 days (to correct remaining injection errors and TCM 1 errors). The

third maneuver is scheduled for M-60 days (for entry targeting), while the final maneuver is planned for M-10 days (to insure the landing conditions are met). Thus the data arc used here begins after the completion of the first two TCM's and will include the third TCM. The solution at the end of data processing will be propagated to encounter, which includes the fourth TCM. The navigation solution, obtained after processing the data from the 105 day interplanetary cruise, will be used to support the final TCM if the maneuver is required. The errors due to the fourth TCM will not affect the navigation solution significantly [9].

The tracking scenario contains data taken from the Deep Space Network (DSN) 34-m High Efficiency (HEF) Deep Space Stations (DSSs) located near Goldstone, California (DSS 15), Canberra, Australia (DSS 45) and Madrid, Spain (DSS 65). The tracking schedule includes one pass of data for each station per week. The tracking passes are started with DSS 15 on the first day, DSS 45 on day four and DSS 65 on day six. After each station makes one pass, six passes (days) are skipped before the next pass at that station is initiated. Thus, DSS 15 will next track on day seven, DSS 45 on day ten and DSS 65 on day twelve. This pattern is repeated until the end of the considered portion of the trajectory. The interval between data points is ten minutes with range and Doppler data collected at the same time. The minimum elevation angles are 50° for DSS 15 and DSS 65, and 30° for DSS 45. Data points for times when the elevation angle is smaller than these values are rejected. All data points that meet the requirements for the day of the pass and the minimum elevation angle are included in the data set. These criteria were set in order to simulate the specified tracking schedule on one 4 hour pass per week at each tracking station during interplanetary cruise [9].

3 Covariance Analysis

The reduction of the estimation errors in the navigation problem is an area of study that has received considerable attention in recent years. one method of improving navigation accuracy is the use of advanced data types, such as Very Long Baseline Interferometry (VLBI). The drawbacks to using advanced data types is their expense due to extensive antenna ti ne requirements and the use of multiple DSN sites simultaneously. For this reason, an effot has been directed at improving the navigation techniques using radio Doppler and ranging data collected using NASA's DSN [7]. The main attraction of these conventional data types is that they are routinely collected in tracking, telemetry and command operations. For example, radio Doppler data is available from communicating with the spacecraft, making this data a free by-product of the communication link. Another advantage of these data types is their long history of use for tracking. This is important since the measurement error models are well developed due to the large set of data from several decades of missions.

In order to improve the navigation accuracy using conventional data types, it is desirable to determine the significant error sources that contribute to the total estimation error on a particular mission. Once the most significant error sources have been identified, more detailed work on those specific error sources can be completed with a goal of reducing their contribution to the overall error. This may be accomplished in many ways, such as improving the mathematical models based on past experience or by using data at different frequencies to reduce frequency dependent errors.

The method used to identify the major error contributors is the so-called *linear covariance analysis [1 O]*. Covariance analysis can be used to study changes in filter

performance due to configuration changes in the filter. Examples include study-
ing the effects of unestimated parameters and using incorrect *apriori* statistics on
the overall state estimation error [1 1]. An error budget, can be developed which
catalogs the contribution] of a particular error source or error source group to the
total navigation uncertainty. The error budget identifies the most significant error
sources for further study. A result easily obtained from the error budget tables is
the sensitivity of the filter to variations in the input parameters. The error groups
considered here consist of spacecraft accelerations due to solar radiation pressure
and small nongravitational accelerations (due to gas leaks, thruster misalignment,
etc), tracking station position errors, refraction due to the troposphere and iono-
sphere, and errors in the Earth orientation (pole motion and $UT1$ errors). These
errors are the major contributors to the estimation error in interplanetary orbit
determination [1 2].

3.1 Error Budget Calculations

in general, the error budget is a summary of the contributions of all error sources
which affect the filter estimate at a specific time, whether modeled explicitly or
not. For this analysis, it is assumed that the filter model and the truth model are
the same. This implies that the filter model is an accurate representation of the
real world.

The model used in the covariance analysis is the same as the model used in
the simulation with the following exceptions. '1 'he covariance analysis included
gravitational effects due to all planets and the Moon, while the simulation con-
siders only central body gravity, In addition, light time corrections were made in
the covariance analysis that were neglected in the simulation. Thus, the covari-
ance analysis results are based on a more accurate model than was used in the

10

simulation.

Error budgets were developed for the Mars 1 'athfinder interplanetary cruise scenario and data schedule described earlier for Doppler-only, ranging-only and Doppler-plus-ranging data sets. The statistics for the orbit determination errors at the end of the tracking were propagated to the nominal time of Mars encounter and expressed in terms of the B-plane coordinate frame [14]. This coordinate frame, also known as the aiming plane, is defined by unit vectors S, T and R. The vector S is parallel to the spacecraft velocity vector relative to the target planet (Mars) at the time of entry into the target planet's gravitational sphere of influence, the vector T is perpendicular to the target planet equatorial plane and the vector R is such that the three unit vectors form a right handed coordinate system. The miss vector B is the aim point for planetary encounter and lies in the T-R plane. The miss vector would be the point of closest approach to the target planet if the target planet did not deflect the flight path of the spacecraft (i.e. the planet had no mass).

The statistics are presented as a 1-σ uncertainty of the miss vector resolved into miss components $B \cdot R$ (normal to the target planet equatorial plane) and $B \cdot T$ (parallel to the target planet equatorial plane), and a 1-σ uncertainty in the linearized time-of-flight (LTOF). The LTOF specifies the time of flight to encounter (point of closest approach) if the magnitude of the miss vector were zero and defines the time from encounter. To convert the 1 TOF to a distance, the hyperbolic approach velocity is required. For the Mars Pathfinder mission scenario, the hyperbolic approach velocity is 5.52 km/s. The miss vector, or the distance from the center of Mars where the spacecraft crosses the target plane, is 4550 km oriented 201.8° clockwise from the T axis [9]. Plots of dispersion ellipses in the B-plane are made for each case to illustrate the contributions of each error

source to the overall error.

Only a summary of the covariance analysis is presented here. More detailed information on this analysis can be found in Burkhart et al [1 3].

3.2 Doppler-Only Case

The error budget results for the Doppler- only case are shown in q'able 2. These results are the magnitudes of the B-plane dispersions about the nominal aim point for planetary orbit insertion for each filter (truth) model error source (in a root-mean-square sense) and for the total filter error. The Doppler case shows that the $B \cdot R$ component of the miss vector is determined to about 25 km and the $B . T$ component of the miss vector is determined to about 20 km. The LTOF is determined to about 7 seconds (about 42 km uncertainly in position). Using 1 Doppler data alone, the result dots not achieve the desired accuracy. However, the accuracy is enough to ensure the safety of the mission [9].

The plot of the 1-σ aiming plane dispersion ellipses for the Doppler-only case is shown in Figure 2. The ellipses shown include the total filter result (all error sources) and the ellipse for each error source individually. The semimajor axis of the filter error ellipse is almost perpendicular to the line connecting the aim point (the origin of the plot) and the center of Mars. The largest contributors to the overall error are the solar pressure, the nongravitational acceleration and the Earth orientation parameters.

3.3 Range-Only Case

The error budget results for the range-only case are shown in Table 3. For this case, the 1?. R component is determined to about 26 km and the $B \cdot T$ component is determined to about 17 km. The LTOF is determined to about 0.6 seconds

(approximately 3 km). From the geometry of the the trajectory (see Figure 1) it can be seen that the Earth-spacecraft range component lies in the plane including the $B \cdot T$ and LTOF directions. The contribution to the overall error budget due to most of the error sources is much smaller than the contribution due to the measurement noise. This is primarily due to the sparse range data collected. Most of the errors in this case will probably be covered up by the measurement noise when adaptation) is attempted.

The plot of the error ellipses for the range- only case appears in Figure 3. The biggest contributors to the overall error are the nongravitational accelerations and measurement noise, with smaller effects due to the solar pressure and troposphere similar in magnitude. Earth orientation is much less important than for the Doppler-on] y case and the measurement noise contributes more to the range-olly errors than to the Doppler-only case. In addition, the nongravitational accelerations contribute more to the overall error for this case than the Doppler-only case. The measurement noise ellipse is oriented slightly differently than the other major error ellipses, which is also different from the Doppler-only case, where the measurement error ellipse was oriented closer to the major error sources. As before, the semimajor axis of the error ellipse is nearly perpendicular to the aim point-Mars equator line.

Due to the mission requirements for Mars Pathfinder, the amount of data collected is much less than in past missions. The contribution to the total error by the measurement noise seems large considering 1 he inherent accuracy of the measurement. By extending the length of the tracking passes in the current scenario to approximately double the number of data points, a significant reduction in the contribution to the total uncertainty due to measurement noise is experienced: a reduction of three kilometers in the $B \cdot R$ direction, half a kilometer in the $B \cdot T$

direction and three quarters of a kilometer in the *LTOF* direction.

3.4 Doppler Plus Range Case

The error budget results for the case where both Doppler and ranging data are used is presented in tabular form in g'able 4. For this case the B . R component of the miss vector was determined to about 17 km and the B .1 component of the miss vector was determined to about 12 km. The LTOF was determined to nearly 0.4 seconds (nearly 2 km in positional uncertainty). As for the other cases, nongravitational accelerations were the dominant error group, with solar pressure, Earth orientation and measurement noise as the next most significant error source groups.

The error ellipses for this case are plotted in Figure 4. The addition of Doppler data raises the error contribution] from Earth orientation a nd ionosphere error groups compared to the range data alone, but Doppler data helps reduce the contribution from the other error source groups except for the range biases and results in a much reduced overall error than range data alone.

From the results obtained, it is clear that the goal of reducing the overall navigation error can be best achieved by concentrating effort on spacecraft accel - erations (solar pressure and random nongravitational accelerations), measurement noise. These errors will be the focus of the adaptive filtering.

4 Adaptive Filtering Approaches

An implicit assumption in the Kahnan filter is that all of the system parameters, including the state transition matrix, the measurement partial derivatives with respect to the state, and the process and measurement noise matrices are known. In general, this is not the case. Often there are parameters not included in the

filter model that influence the measurements, This results in a modeling mismatch between the filter and the measurements which affects tile state transition matrix and the mea su rement partials. in addition, the process noise and measurement noise matrices are rarely precisely known. For these reasons, it may be desirable to apply an adaptive filtering scheme to tile problem at hand.

The general problem to be solved is described by

$$z_{i+1} = \Phi_i z_i + u_i$$

$$y_i = H_i z_i + v_i$$

where z_i is the state vector, Φ_i is the state transition matrix, u_i is the process noise vector, v_i is the measurement noise vector and H_i is the measurement matrix. Both u_i and vi are uncorrelated zero-mcall Gaussian white noise sequences with

$$E\{u_i\} = 0, \qquad E\left\{u_i u_j^T\right\} = Q\delta_{ij},$$

$$E\{v_i\} = 0, \qquad E\left\{v_i v_j^T\right\} = R\delta_j,$$

where Q is a nonnegative definite matrix and R is a positive definite matrix, both with unknown true values. The standard filtering problem is to estimate z_i based on the observation set Y* $=$ $\{y_1, y_2, \ldots, y_i\}$, where the estimated values will be denoted $\hat{z}_i$. In this case, the discrete Kalman filter is used:

$$\hat{z}_{i+1}^{(-)} = \Phi_i \hat{z}_i^+$$

$$P_{i+1}^{(-)} = \Phi_i P_i^{(+)}\Phi_i^T + Q$$

$$\hat{z}_i^{(+)} = \hat{z}_i^{(-)} + K_i\left(y_i - H_i\hat{z}_i^{(-)}\right)$$

$$K_i = P_i^{(-)}H_i^T\left(HP_i^{(-)}H_i^T + R\right)^{-1}$$

$$P_i^{(+)} = (I - K_iH_i)P_i^{(-)}$$

where K_i is the Kalman gain and $vi = y_i -- H_i\hat{z}_i^{(-)}$ is the measurement residual with covariance $HP_i^{(-)}H_i^T + R$. This solution is optimal based on exact knowledge

15

of Q and R. However, since this is not the case here, an adaptive filter will be used to help determine input values for Q and R

The first step in selecting an adaptive filtering scheme is to study the techniques available. Based on the discussion present ed by Mehra in 1972, adaptive filtering methods can be divided into four groups: maximum likelihood, correlation covariance matching and Bayesian [15]. Covariance matching techniques will not,)e discussed here.

4.1   Evaluation of Adaptive Methods

Three main adaptive estimation approaches were evaluated during this study. The details of an extensive literature survey can be found in Burkhart [16].

The first approach investigated was a maximum likelihood method proposed by Meyers and Tapley [1 7]. This approach utilizes a so-called Adaptive Limited Memory Filter (ALMF) which involves the formulation of unbiased estimates for the noise variances and covariances (both are assumed nonzer o in the paper) and computing estimates sequentially based on a user-specified set of data. The Meyers and Tapley approach does not appear to offer a significant improvement over the current operational approach in terms of making the tuning process more systematic.

The second approach tested was an innovation correlation approach formulated by Mehra [1 8]. The original Mehra formulation, which is for a linear time invariant problem, was tested on the Mars Pathfinder interplanetary orbit determination problem. When the system has small time variations, the approach is generally robust enough to be effective. However, in the orbit determination problem, the measurement matrix H_i has large variations over each tracking pass and from one pass to the next. As expected, the results from direct application of Mehra's scheme

were not very good. Mehra's scheme was then re-formulated as part of this study for time-varying systems and applied to the interplanetary orbit determination problem, again without good results. Other authors (including Bélanger [1 9]) have generalized Mehra's scheme for time-varying stationary problems without good results. This method is apparently best suit cd for time invariant problems, and is not applicable to the interplanetary orbit determination problem.

The final approach evaluated was a Bayesian method formulated by Magill [1]. The approach is to implement a bank of Kalman filters, each modeled with different values of a finite unknown parameter set. The method, in its original form, computes the weighted sum of the estimates from each filter to determine the optimal adaptive estimate. Another way tile Magill filter has been applied is as a multiple hypothesis tester. Jn this use, the output of interest is the weight for each filter in the bank, which is used to determine which hypothesized filter in the bank is the correct one [5].

4.2 Adaptive Kalman Filter Bank Development

Based 011 the literature review and preliminary simulation studies, the adaptive estimator implemented in this work is the adaptive scheme first introduced by Magill [1], This method is known as simply the Kalman filter bank or the Multiple Mode] Estimation Algorithm (MM EA), shown in Figure 5 [5]. The main reason this approach was selected is that it solves this particular problem well. In addition, there are no restrictions beyond those required for use of the Kalman filter that are required to implement this approach [6], Finally, this approach fits quite well with the current orbit determination approaches in use for interplanetary navigation. Implementation of this approach will not require a new filtering methodology or extensive modification to the current filter.

17

The problem to be solved may be stated as follows: An estimate is desired for a sampled-data, Gaussian process, which may be corrupted by additive noise, such that the estimate minimizes some performance measure. The observed process is a function of some unknown parameter vector, α, which is a member of a finite set of known parameter vectors [1].

Assume that the parameter vector α is a random variable that may or may not be Gaussian. This implies that α is an unknown constant for a specific sample run, but has a known statistic] distribution, The optimal estimate $\hat{z}_k$ is a weighted sum of the individual Kalman filters, with each filter operating with a different value of α. The weighted sum is given by

$$\hat{z}_k = \sum_{i=1}^{L} \hat{z}_k(\alpha_i) p(\alpha_i | y_k^*) \tag{1}$$

where $p(\alpha_i | y_k^*)$ is the discrete probability for α_i conditioned on the measurement sequence y_k^*. The problem now is reduced to the determination of the weight factors $p(\alpha_1 | y_k^*), p(\alpha_2 | y_k^*)$, etc. As the measurement -process evolves, these values will change with each step recursively. As more measurements are processed, tile knowledge of the state and the unknown parameter α will increase. If as time progresses it is possible to learn which stochastic process is observed, then it is reasonable to expect the optimal estimator to converge to the appropriate filter for that process. In terms of the block diagram in Figure 5, the weighting coefficient for the true filter will converge to one while all of the rest will converge to zero []], [20].

The weighting factors $p(\alpha_i | y_k^*)$ are the adaptive feature of this estimator [1]. Using Hayes' rule, the weights are computed via

$$p(\alpha_i | y_k^*) = \left[\frac{p(y_k^* | \alpha_i) p(\alpha_i)}{\sum_{j=1}^{L} p(y_k^* | \alpha_j) p(\alpha_j)} \right], \qquad i = 1, 2, \ldots, L. \tag{2}$$

The values for $p(\alpha_i)$ are assumed known, so all the terms in this relation are known except for $p(\mathbf{y}_k^*|\alpha_j)$. To compute the value for $p(\mathbf{y}_k^*|\alpha_j)$, the processes $\mathbf{x}$ and $\mathbf{y}$ will be assumed to be Gaussian. In addition, the measurement sequence $\mathbf{y}_k^*$ will be assumed to be a sequence of scalar measurements $y_0, y_1, \ldots, y_k$. When these conditions are applied, the result is

$$p(\mathbf{y}_k^*|\alpha_j) = \frac{1}{\sqrt{2\pi \left(H_k P_k^- H_k^T + R_k \right)}} \exp\left[-\frac{1}{2} \frac{\left(y_k - H_k \hat{z}_k^- \right)^2}{\left(H_k P_k^- H_k^T + R_k \right)} \right] p(\mathbf{y}_{k-1}^*|\alpha_j) \quad (3)$$

In general, $p(\mathbf{y}_k^*|\alpha_j)$ will be different for each filter in the bank.

In the Mars Pathfinder problem, only the apes.teriori probabilities $p(\alpha_i|\mathbf{y}_k^*)$ for each hypothesis are computed by the filter bank. As the filter bank processes data, the weighting factor for the best filter will increase while the other weighting factors decrease [5]. For this problem, the Kalman filters are assumed to have an unknown measurement noise variance, in addition to possibly unknown process noise parameters. All other parameters and models between the filter and the environment are the same. Thus the MMEA will be determining the filter with the parameters that are the closest to the values from the environment, as determined from the measurements.

5 Results

Results from severa: sets of cases are shown. The first set of results are for range cases where all noise parameters are included in tile filter, but only a selected group of parameters are adaptively determined. The case presented here is for adaptation of measurement noise and NGA parameters. In addition to the range cases, several cases where Doppler data is processed are shown. The final case shown involves a change in the nongravitational parameter during tracking. Range data is utilized in this study along with a high-gain antenna, which reduces the random noise

component of the noise profile. 'I'his allows the Kalman filter bank to run over a larger set of data [1 6].

All results presented arc for range measurements only and for Doppler measurements only. The weighting coefficients for each filter in the bank arc presented in the encounter plane along with the estimates, computed error covariances and true values. All error ellipses plotted for the filter bank results show 1 -σ errors. The ellipses for the simulation results arc oriented differently than those for the error budget analysis due to the inclusion of planetary gravity in the analysis, which was not included in the Mars Pathfinder simulation.

5.1 Range Case

The first case considered adapts the non gravitational accelerat ion parameters and the measurement noise parameter. A bank of 15 Jilters is set up with the scaling from the nominal values as shown in Table 5. The filter numbers are determined as shown in the table. For example, filter 14 has a measurement noise that is ten times the nominal value and a NGA steady-state variance that is five times the nominal value.

The weighting factors for this scenario are plotted in Figure 6. This plot shows nonzero weights for filters 6, 7 and 8. The weight for filter 8 is nearly unity, while the other filters have negligible weights. The filters in the bank that do not have the correct measurement noise parameter arc eliminated quickly by the MMEA, with the remaining data before a bank is chosen used to differentiate the process noise values for the filters with the correct measurement noise parameter.

The encounter plane estimates and covariances for filters 6 through 10 arc shown in Figure 7. For this case, filters 6 and 7 appear to be quite close to the truth. Filter 8, with a slightly higher weight and the correct filter, had slightly

worse estimates. Since these results are based on a single realization of the random processes, Monte Carlo analysis with different realizations of the random processes was conducted to verify the expected results. These Monte Carlo results are presented in Burkhart [1 6].

5.2 Doppler Case

The Doppler case adapts the nongravitational acceleration parameters and the measurement noise parameter. A bank of 15 filters is set up with the scaling from the nominal values as shown in Table 5 for the range case.

The weighting factors for this scenario as-e plotted in Figure 8. This plot shows nonzero weights for filters 11 to 15. The weight for filters 11 and 12 are approximately 0.4, while filter 1 3 has a weight near 0.25 and filters 14 and 15 have weights of shout zero. As before, the correct filter is filter 8. 'J'bus, for this case, the filter does not converge to the correct filter. These results for the Doppler case arc not as conclusive as for the range case. Problems with the formulation of the Doppler measurement due to linearization and the differenced range formulation are apparent from the results. The filter chosen by the filter bank has similar or smaller process noise and larger measurement noise compared to the environment.

The encounter plane estimates and covariances for filters 8 and 11 through 15 are shown in Figure 9. For this case, filter 8 appears to be the best filter.

5.3 Study of Noise Parameter Variations

The final run presented involves simulated data with a change in the nongravitational acceleration steady-state variance after approximately half of the tracking segment is complete. The parameter change represents a possible valve leak after

a TCM or some other change in the force profile of the spacecraft. This variance is assumed constant for the first part of the tracking. After 62 days of tracking, or just after the Mars Pathfinder TCM 2, the parameter is changed to a new constant value. This situation represents the effect of a thruster leaking after it is fired for the TCM, a leak in a fuel line, or some other phenomena related to a thruster malfunction. The process noise term is scaled by 10, which corresponds to scaling the NGA variance by $\sqrt{10}$. The scaling was chosen to be such that the correct filter (after the variance change) is no longer part of the bank of 15 filters (see 'Table 5). In this way, the case will illustrate that the bank will converge to the filter operating the closest to the data's noise profile. All error sources are included in the simulation.

The weighting factors for each filter are shown in Figure 10. For the first 60 days of tracking, the filter is converging to filter 8, which is the correct filter. After the change in the variance, the filter quickly selects filter 9, which has nominal values for all variances except a scaling on the NGA of 5. It is thus shown that the bank is able to detect changes due to unmodeled thruster variations.

6 Summary

The adaptive Kalman filtering methodology was developed using the enhanced Kalman filter and the Magill filter bank. The approach was used to adaptively determine the steady-state noise variances in the states for the Mars Pathfinder interplanetary cruise mission. Tracking scenarios used in the adaptive study included range only and Doppler only data. The cases studied were determined based on the error budget results, where the most significant errors for each tracking scenario were found.

Results for the range cases show that the adaptive algorithm chooses the filter

with the same parameters as the simulated data. Cases where there was no clear winner were shown to have several filters with nonzero weights and similar performance. Smaller error sources are more difficult to determine, leading to selection of no single filter, but rather several with similar performance. Based on these results, the filter bank will be a useful tool in the tuning process for the operational filter. In addition, the bank is useful for the determination of changes in the tracking data, giving some warning of potential problems such as a thruster malfunction or some other change in the accelerat ion profile of the spacecraft.

Results for the Doppler cases are less conclusive. One problem with this formulation of the Doppler measurement is the effect of roundoff errors due to the linearization and the differenced range formula. For example, the range values are on the order of 108 km. The measurement noise on the Doppler measurement is 0.01 mm/s, or 10^{-8} km. The difference is 16 digits, or near the numerical limits of a 64 bit number. In addition, the differenced range formulation implemented in the partial derivatives and the data generation may be susceptible to differences due to Earth rotation from the start to the end of the tracking pass. One way to address these problems is to implement a more theoretically correct version of the range rate measurement. In addition, an extended Kalman filter, which dots not involve a linearization about a reference trajectory, may help this problem as well. The 1 Doppler results in genera] show that filters with larger measurement noise are chosen, while the other filters have zero weights. In most cases, the filters with correct or smaller process noise are chosen, as for the range case.

A next step is implementation of the filter bank for use in processing actual mission data. The proposed method could be used by the navigation team members making the individual runs to systematically eliminate incorrect filter models. This could be completed by several individuals independently, with comparison of

results after processing is complete.

One additional advantage is the obvious parallel computing possibilities with this approach. This approach can be implemented using search methods (such as genetic algorithms) to update the filter bank for operation in an iterative fashion. These genetic algorithms can be implemented easily using the filter bank and can be implemented in a parallel processing environment.

The Kalman filter bank is a method that has a successful history in real-time applications such as power system fault detection, image processing and terrain-height correlation for helicopter navigation. It has been shown here to also have application in interplanetary orbit determination.

7 Acknowlegdements

8 **References**

[1] Magill, D. T., "Optimal Adaptive Estimation of Sampled Stochastic Processes," *IEEE Transactions on Automatic Control*, Vol AC-10, No. 4, October, 1965, pp. 434-439.

[2] Brown, R. G. and Hwang, P. Y. C., "A Kalman Filter Approach to Precision GPS *Geodesy," Navigation, Journal of the Institute of Navigation,* 30:, No. 4, Winter 1983-84, pp. 338-349.

[3] Mealy, G. 1,., "Application of Multiple Model Estimation to a Recursive Terrain 1 leight Correlation System," *IEEE Transactions on A utomatic Control*, Vol. AC-28, No. 3, March, 1983, pp. 323-331.

[4] Girgis, A. A. and Brown, R. G., "Adaptive Kalman Filtering in Computer Relaying: Fault Classification using Voltage Models," *IEEE Transactions on Power Apparatus and System*, Vol. PAS- I 04, No. 5, May, 1985, pp. 1168-1177.

[5] Brown, Robert G. and Huang, Patric Y. C., *Introduction to Random Signals and Applied Kalman Filtering*, Second Edition, John Wiley and Son S, 1992, pp. 398-402.

[G] Brown, R. G., "A New Look at the Magill Adaptive Filter as a Practical Means of Multiple Hypothesis Testing," *IEEE Transactions on Circuits and Systems*, Vol CA S-30, No. 10, October, 1983, pp. 765-768.

[7] Estefan, J. A., Pollmeier, V. M. and Thurman, S. W., "Precision X-Band Doppler and Ranging Navigation for Current and Future Mars Exploration Missions," *Advances in the Astronautical Sciences*, J. Teles and M. V. Samii, Editors, Vol. 84, Part 1, pp. 3-16, 1993.

[8] Bhaskaran, S., Thurman, S. W. and Pollmeier, V. M., "Demonstration of a Precision Data Reduction Technique for Navigation of the Galileo Spacecraft", *Advances in the Astronautical Sciences*, J. E. Cochran et al., Editors, Vol. 87, Part 11, pp. 785-798, 1994.

[9] Kallemeyn, 1'., "Pathfinder 1'reject Navigation Plan - Critical Design Review Version," *JPL Document D-11349* (Internal Document), July, 1994.

[1 O] Gelb, A., *Applied Optimal Estimation,* MIT Press, 1974.

[11] Bierman, G. J., *Factorization Methods for Discrete Sequential Estimation,* Academic Press, 1977.

[12] Jordan, James F., Madrid, George A. and Pease, Gerald E., "Effects of Major Error Sources on Planetary Spacecraft Navigation Accuracies", *Journal of Spacecraft and Rockets,* Vol. 9, No. 3, March, 1972, pp. 196-204.

[13] Burkhart, P. 11., Bishop, R. II. and Estefan, J. A. "Covariance Analysis of Mars Pathfinder interplanetary Cruise", *Advances in the A stronautical Sciences,* II. Jacobs, Series Editor, Vol. 89, 1995.

[14] Kizner, W., "A Method of Describing Miss Distances for Lunar and Interplanetary Trajectories," *JPL External Publication No. 674,* August 1, 1959.

[15] Mehra, Raman K., "Approaches to Adaptive Filtering," *IEEE Transactions on Automatic Control,* October, 1972, pp. 693-698.

[16] Burkhart, P. D., "Adaptive Orbit Determination for Interplanetary Spacecraft," Ph.D. Dissertation, The University of Texas at Austin, May, 1995.

[17] Meyers, Kenneth A. and Tapley, Byron D., 'Adaptive Sequential Estimation with Unknown Noise Statistics," *IEEE Transactions on Automatic Control,* August, 1976, pp. 520-523.

[18] Mehra, Raman K., "On the identification of Variances and Adaptive Kalman Filtering," *IEEE Transactions on A utomatic Control,* Vol. AC-15, No. 2, April, 1970, pp. 175-184.

[19] Bélanger, Pierre R., "Estimation of Noise Covariance Matrices for a Linear Time-Varying Stochastic Process," *Automatica*, Vol. 10, May, 1974, pp. 267-275.

[20] Hilborn, C. G., Jr. and Lainiotis, D. G., "Optimal Adaptive Filter Realizations for Sample Stochastic Processes with an Unknown Parameter," *IEEE Transactions on Automatic Control,* Vol AC-14, 1 December, 1969, pp. 767-770.
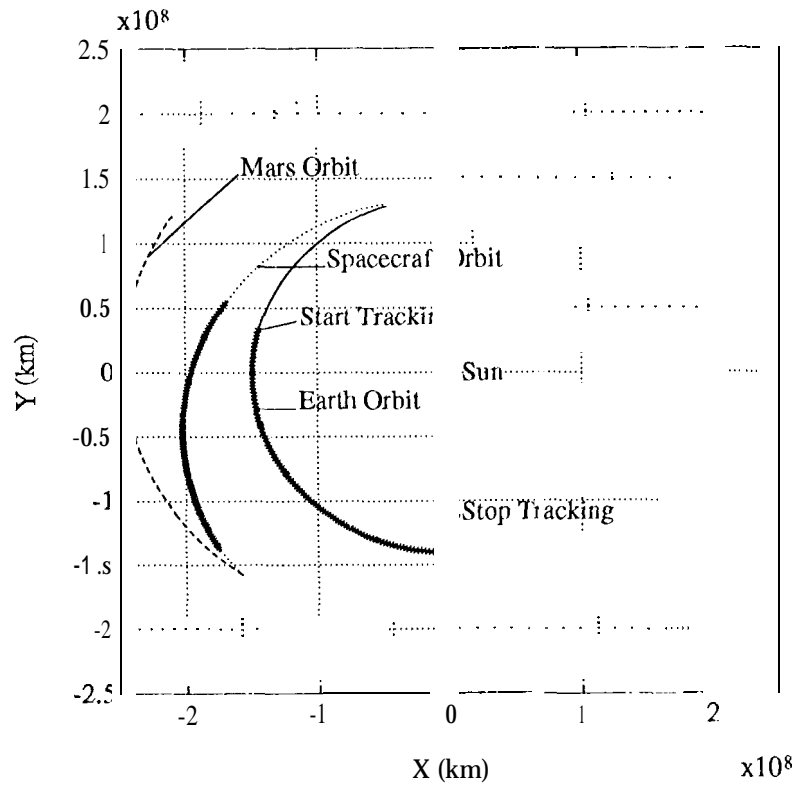
Figure 1: Mars Pathfinder Trajectory (planar projection)

Table 1: Mars Pathfinder trajectory characteristics (March 5-June 18, 1997)

Parameter	Value (start to end of arc)
Earth to spacecraft range (km)	36.2×10^6 to 180×10^6
Geocentric Declination (deg)	15.85 to --0.12
Sull-1tartll-1'robe (SEP) angle (deg)	1.4 to 51.7

Table 2: Error Budget -Doppler Measurements

Error Source	$B \cdot R$ (km)	$B \cdot T$ (km)	LTOF (see)
Epoch State	0.001	0.005	0.003
SRP Parameters	10.692	10.454	6.829
Nongrav Accel.	18.252	13.633	2.822
ionosphere	1.917	1.297	0.189
Troposphere	5.625	3 1 5	0.577
Station locations	5.263	4.484	0.534
Earth Orientation	9.121	5.542	1.0"31
Measurement Noise	7.102		0.751
RSS Total	25.379	20.260	7.542
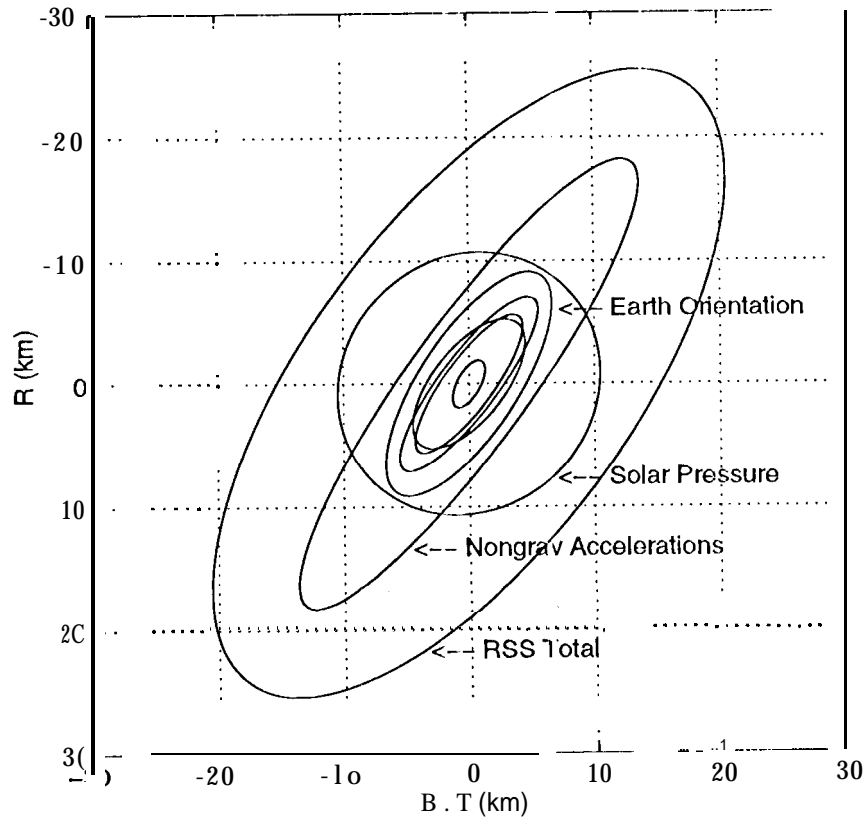
Figure 2: Aiming Plane Dispersions (1-a) Doppler data

Table 3: Error Budget - Range Measurements

Error Source (km)	$B \cdot R$ (km)	$B \cdot T$ (km)	LTOF (sec)
Epoch State	4.76e --44	3.52e =4	5.38e --6
SRP Parameters	8.858	7.179	0.222
Nongrav Accell.	19.615	12.667	0.369
Ionosphere	0.220	0.147	0.007
Troposphere	7.001	4.127	0.097
Station Locations	5.075	4.162	0.170
Earth Orientation	1.652	1.041	0.057
Range Biases	4.549	1.776	0.140
Measurement Noise	11.593	5.836	0.321
RSS TTotal	26.397	16.880	0.591
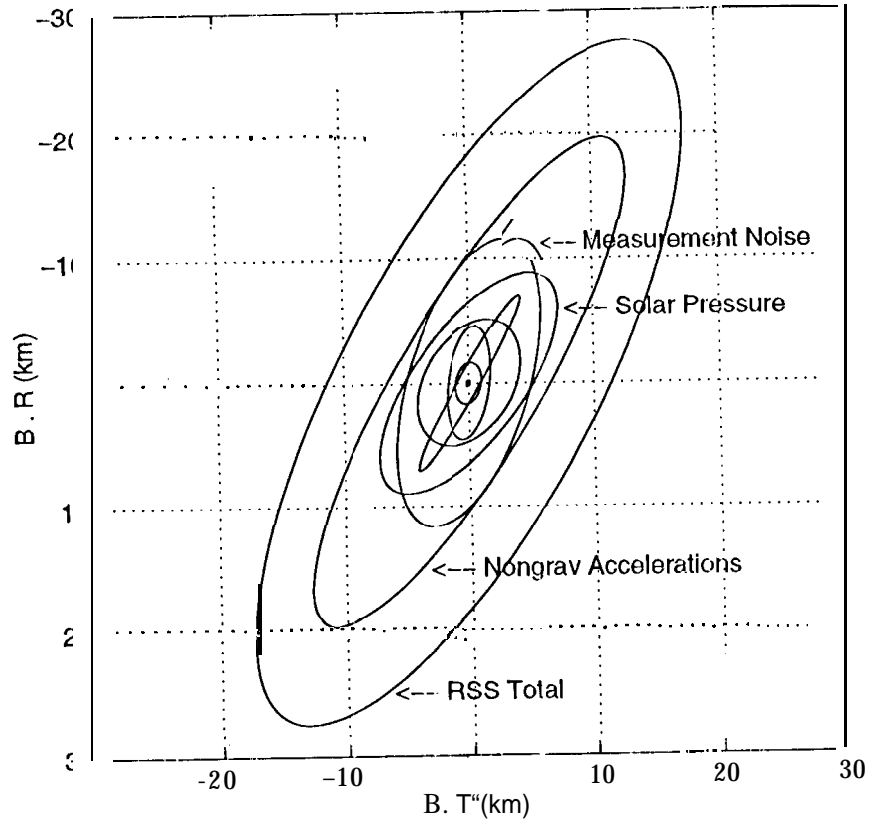
Figure 3: Aiming Plane Dispersions $(1\text{-}\sigma)$ - Range data

Table 4: Error Budget - Doppler Plus Range Measurements

Error Source	$B \cdot R$ (km)	$B \cdot T$ (km)	LTOF (sec)
Epoch State	$3.8e-5$	$3.5e-5$	$4.8e-7$
SRP Parameters	5.941	3.759	0.123
Nongrav Accel.	13.299	8.533	0.243
Ionosphere	1.138	0.712	0.016
Troposphere	2.171	1.648	0.040
Station Locations	2.385	2.346	0.101
Earth orientation	5.585	3.870	0.141
Range Biases	4.464	3.134	0.043
Measurement Noise	5.606	4.075	0.063
RSS Total	17.504	1 1.71r	0.335
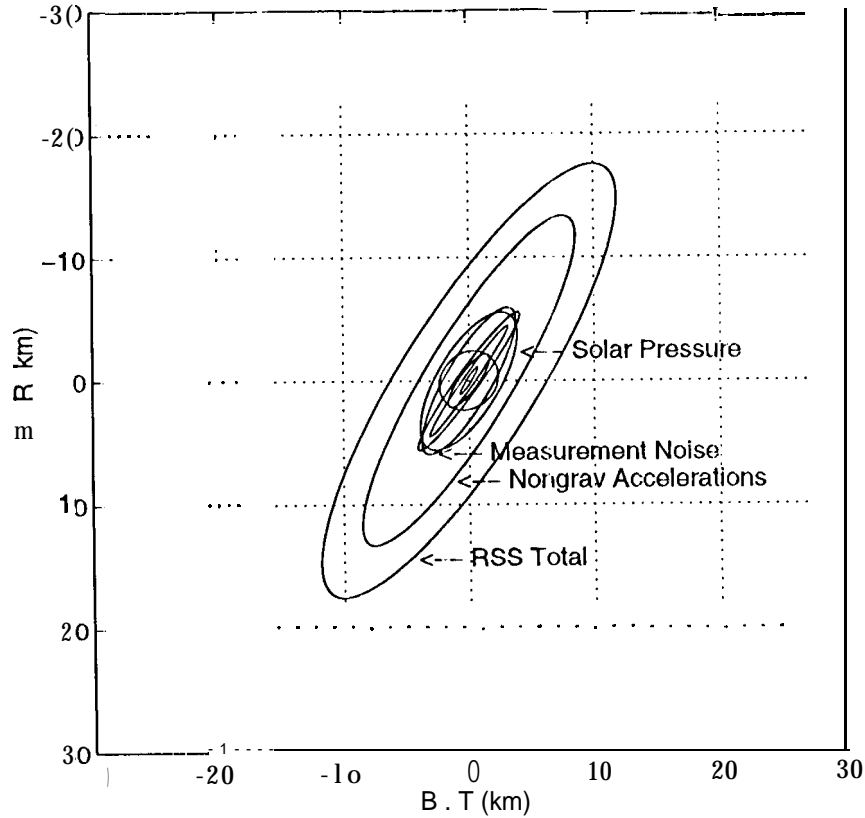
Figure 4: Aiming Plane Dispersions (1-σ) - Doppler Plus Range data
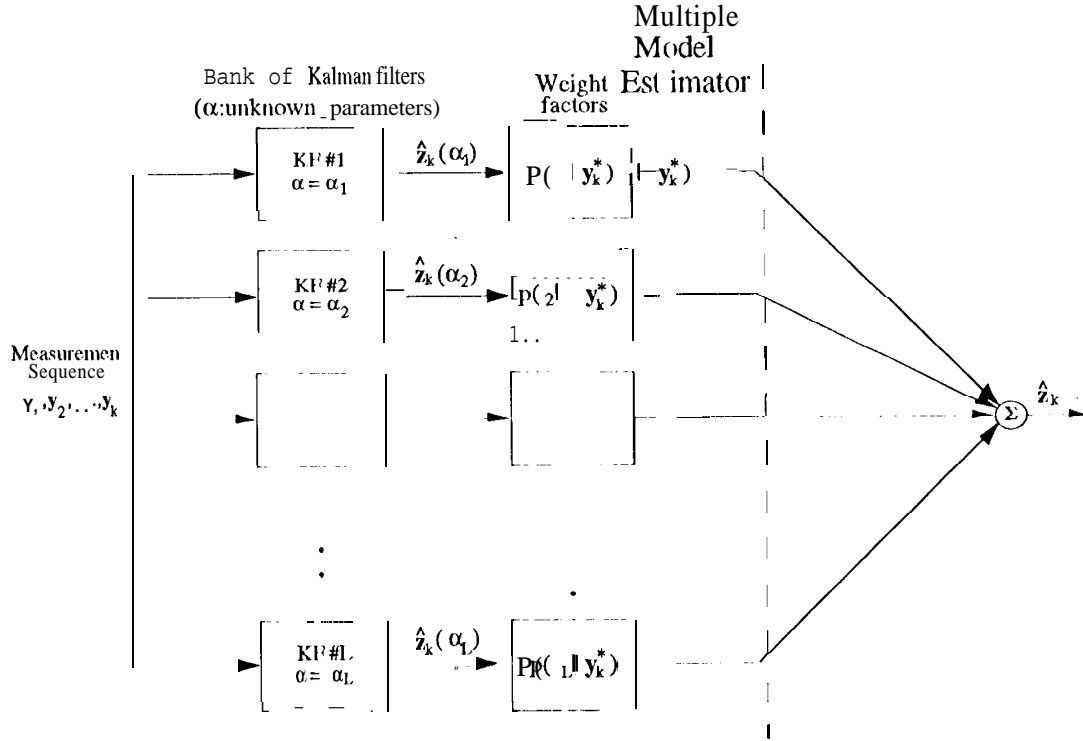
Figure 5: Weighted Sum of Kalman Filter Estimates

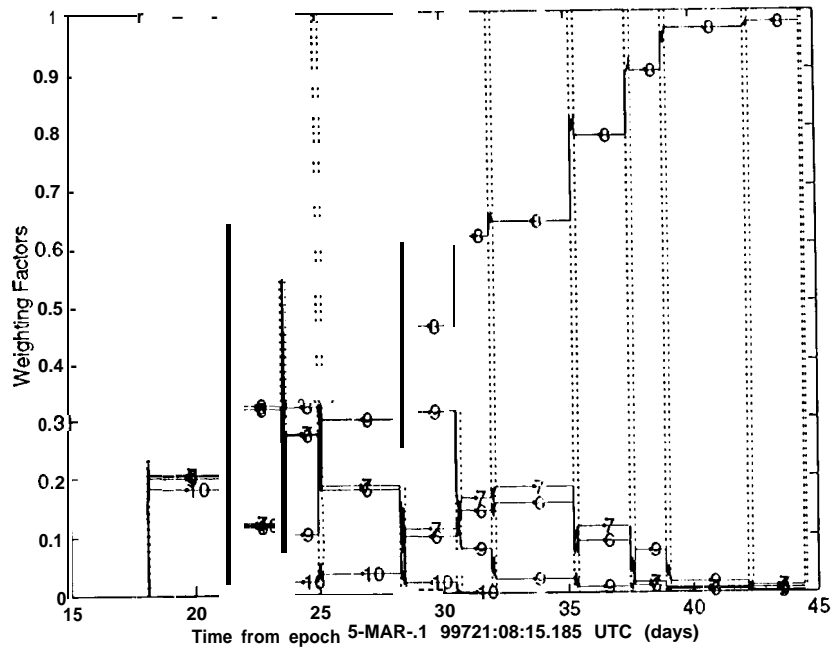| NGA Scaling	Filter Number		
0.1	1	6	11
0.2	2	7	12
1.0	3	8	13
5.0	4	9	14
10.0	5	10	15
	0.1	1.0	10.0
	Measurement Noise Scaling		

Table 5: Scaling factors: Measurement and NGA Parameters

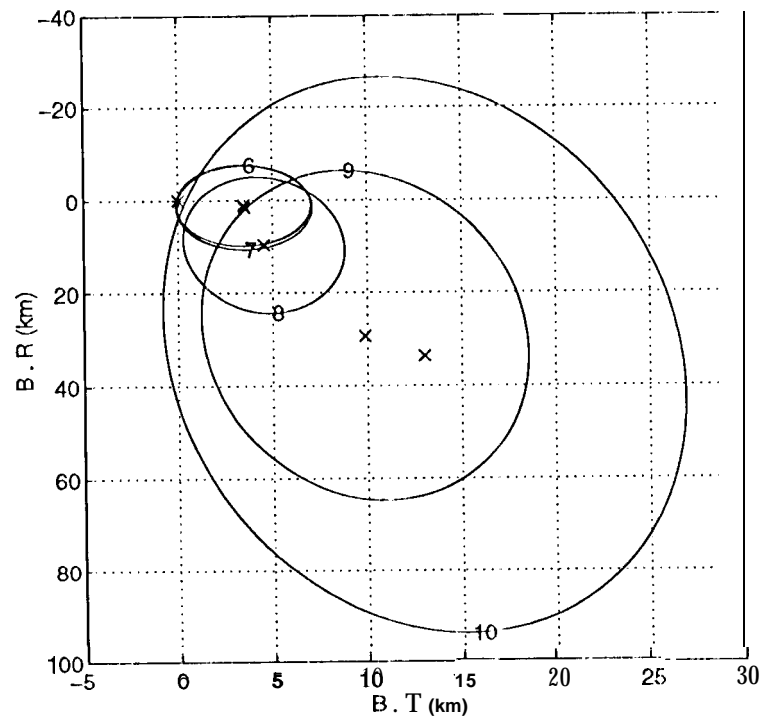Figure 6: Weighting Coefficients - Measurement and N GA Parameters Adapted

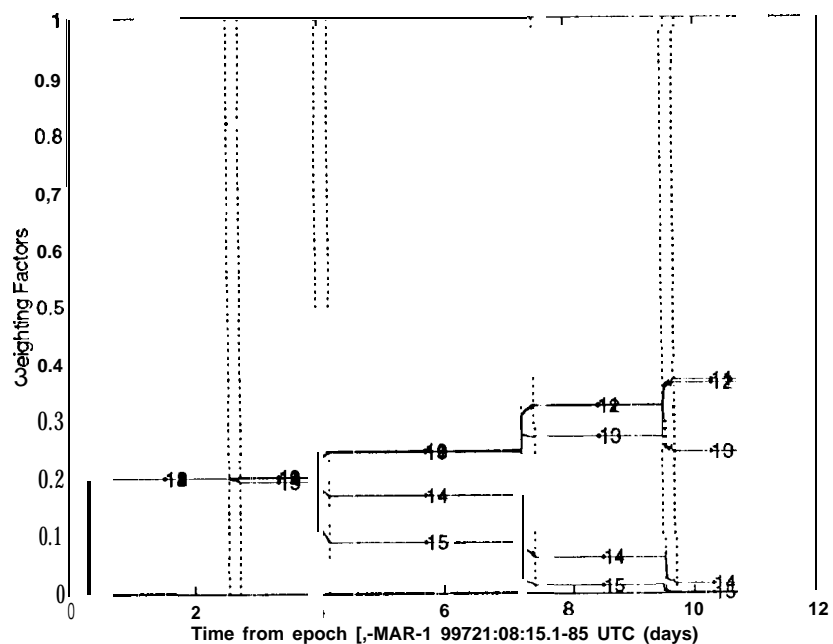Figure 7: Encounter Results - Measurement and NG A Parameters Adapted

Figure 8: Weighting Coefficients - Measurement and NGA 1 Parameters Adapted (Doppler)
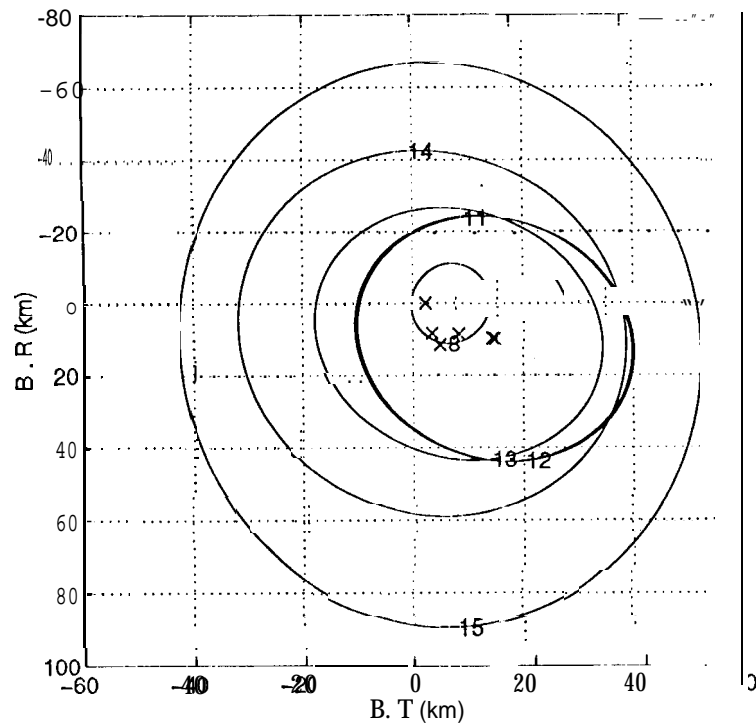

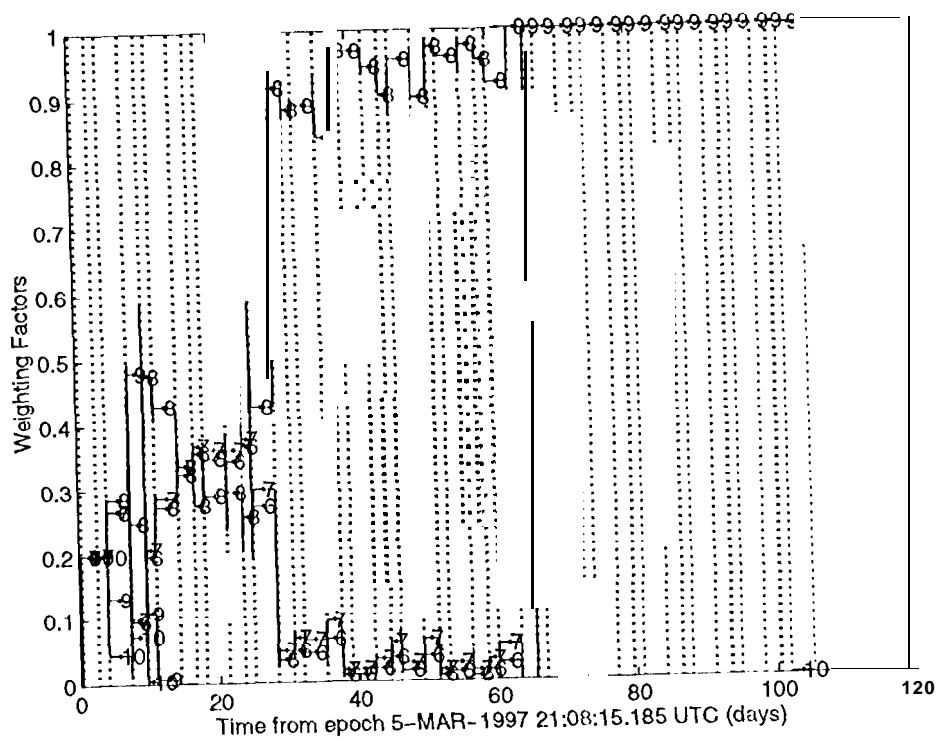Figure 9: Encounter Results -- Measurement and NGA Parameters Adapted Case (Doppler)

Figure 10: Weighting Coefficients - NGA Parameter Change (HGA)